

# Chapter 3

## Structure-Properties Relationships

Dr. Wallace Matizamhuka

**Abstract** This chapter explores the correlations between the microstructures of hard, superhard and ultrahard materials and resulting properties. Key microstructure features and their effect on mechanical properties (hardness, fracture toughness, strength, wear and thermal properties) are discussed. A number of analytical and empirical structure-properties-behaviour model(s) are proposed for a range of hard, super and ultrahard materials, extending from classical theories such as the Hall-Petch relationship, theory of critical distance and formation of Griffith cracks. The challenge in extending these theories to nanostructured materials is also discussed. Furthermore, the chapter addresses, the ‘strength-toughness conflict’ in hard, super and ultrahard materials and the effect of microstructure on crack growth behaviour. Some useful techniques that have been utilised to counteract the conflicts between strength and fracture toughness are also highlighted. The chapter also serves as an introduction to the later chapters where techniques for microstructure analysis and property testing are discussed in greater detail (Chap. 5). In Chap. 6 an in-depth discussion of nanostructured materials and the effect on material properties such as hardness, as well as their industrial applications, are presented.

### 1 Introduction

Hard, superhard and ultrahard materials display exceptional mechanical performance in hardness, toughness, incompressibility, thermal conductivity and wear resistance. This makes them suitable candidates in a wide range of applications such as mining industry drilling bits in rock cutting and petrochemical industry, polishing tools and machining tools for advanced aerospace alloys. A more detailed discussion of these and other applications of superhard and ultrahard materials is presented in Chap. 2. During operation, the tools are subjected to high-temperature

---

Dr. W. Matizamhuka (✉)

Senior Lecturer, Department of Metallurgical Engineering,  
Vaal University of Technology, Vanderbijlpark, South Africa  
e-mail: [walamatiza@yahoo.co.uk](mailto:walamatiza@yahoo.co.uk)

wear and multiple interrupted impacts. Despite the superior mechanical properties, these materials are bound to fail mostly through chipping and fracture owing to their brittle behaviour, i.e. low fracture toughness. As in all materials, their performance is closely linked to the microstructure and obviously the operating conditions.

Although diamond has sufficed as the hardest material known to man, its interaction with iron-containing alloys at elevated temperatures limits its industrial application to machining of non-ferrous and non-metallic materials. In the 1960s a synthetic superabrasive cubic boron nitride (c-BN) was introduced in the market (Zheng et al. 1999; Solozhenko et al. 2005; Pierson 1994; Riedel 1992, 1994; Haines et al. 2001; Brazhkin 2007; Leger et al. 1994; Zerr and Riedel 2000; Badzian 1981; Nakano et al. 1994; Knittle et al. 1995; Nakano 1996; Zhao et al. 2002; Komatsu et al. 1996). The value of c-BN as a superabrasive lies in its much higher oxidation stability compared to diamond and its nobility to iron attack at elevated temperatures. However the hardness of c-BN is about half that of diamond. Over the years several attempts have been aimed at filling the hardness gap between the two traditional superabrasives (Matizamhuka 2010). This has been driven by the need to obtain an all-purpose, cost-effective superabrasive with a wider range of applications. A ‘superhard’ material by convention is one whose hardness exceeds 40 GPa on the Vickers scale of hardness. In this regard, only diamond and cubic boron nitride (c-BN, hereafter) qualify for this title.<sup>1</sup> However, over the years there have been tremendous efforts in the search for potential ‘superhard’ materials (Solozhenko et al. 2005; Pierson 1994; Riedel 1992, 1994; Haines et al. 2001; Brazhkin 2007; Leger et al. 1994; Zerr and Riedel 2000; Badzian 1981; Nakano et al. 1994; Knittle et al. 1995; Nakano 1996; Zhao et al. 2002; Komatsu et al. 1996). This has been stimulated by the need to design materials which not only approach diamond in hardness but are more useful and complimentary to the traditional superhard materials (Solozhenko et al. 2005; Pierson 1994; Riedel 1992, 1994; Haines et al. 2001; Brazhkin 2007; Leger et al. 1994; Zerr and Riedel 2000; Badzian 1981; Nakano et al. 1994; Knittle et al. 1995; Nakano 1996; Zhao et al. 2002; Komatsu et al. 1996). To design hard and superhard materials, it must be understood what makes these exceptional materials special. The link between structure and performance of these materials has been utilised to produce some of the most promising and important superhard materials. Thus it is imperative to understand such relationships in order to successfully develop future functional superhard materials. The review below is not meant to be completely exhaustive but to give an insight on the influence/role that microstructural features play on material performance. This chapter also serves as an introduction to the later chapters where techniques for microstructure analysis and property testing (Chaps. 4 and 5) and nanostructured materials and effect on

---

<sup>1</sup> Diamond can also be considered as ultrahard. Ultrahard materials are those whose hardness exceeds 80GPa on the Vickers scale of hardness.

materials properties as well as their industrial applications (Chap. 6) are discussed in greater detail.

## 2 Designing Superhard Materials

The synthesis of materials with hardness comparable to diamond has gained fundamental technological interest over the years (Zheng et al. 1999). This has emanated from the need of obtaining materials which are more useful rather than ‘harder than diamond’ as highlighted earlier (Solozhenko and Gregoryanz 2005). This may include materials that are expected to be chemically and thermally more stable than diamond and harder than c-BN. However to design new ‘superhard’ materials, it must be understood what makes diamond special. It is a well-known fact that the diamond crystal structure consists of tetrahedrally bonded  $sp^3$ -hybridised carbon atoms forming a rigid three-dimensional covalent network of high symmetry with extreme resistance to shear (Pierson 1994). There exist other carbon-based materials with shorter and stronger bonds than those in diamond (e.g. graphite), but these do not form a three-dimensional covalent network as in diamond, rather these carbon networks are associated with bonding which is heterodesmic in nature, in which layers are linked by strong covalent bonds and separated by weak interlayer forces (Van der Waals) (see Fig. 3.1) (Pierson 1994). A three-dimensional network composed of short, strong bonds is thus critical for hardness. The short bond length implies a high atomic and mass density comparable with diamond. Furthermore, a material is considered hard if it resists both elastic and plastic deformation (Riedel 1992; Haines et al. 2001). In principle, plastic deformation involves permanent and irreversible motion of atoms with respect to each other, often through the creation and movement of dislocations (Haines

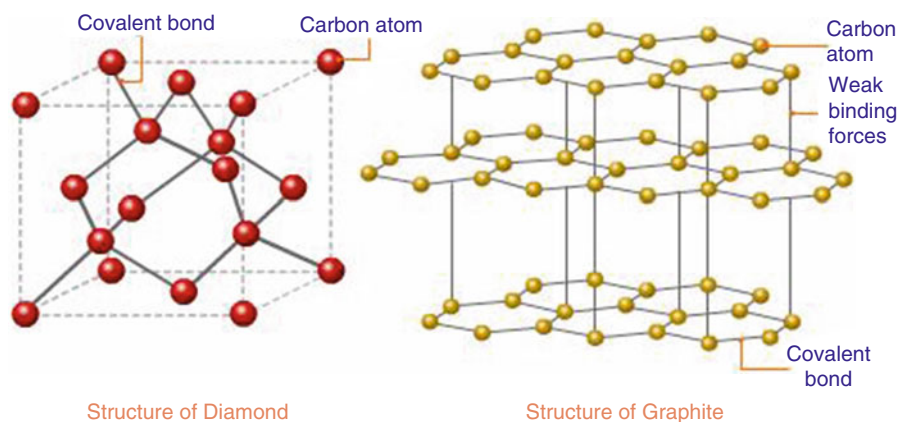


**Fig. 3.1** Schematic representation of a diamond  $sp^3$ -hybridised bonds in comparison to the layered graphite structure (chemistry.tutorvista.com)

et al. 2001). This is in contrast with elastic deformation where atoms revert back to their initial positions after removal of load. Thus highly directional and strong bonding is of great importance in opposing or resisting such motions. However microscopic parameters (i.e. type of atom, structure and atomic forces) alone do not govern the mechanical characteristics of a material but also the morphology of the material constituents, defects in the sample, methods of measurement and temperature play crucial roles (Haines et al. 2001; Brazhkin 2007).

Furthermore, the strategic search for new superhard materials has also been directed towards modification of grain morphology and the state of defects to approach high hardness values (Haines et al. 2001; Brazhkin 2007). Another consideration in the designing of superhard materials is based on the stiffness of a material which is basically a measure of the resistance to volumetric compression (bulk modulus,  $B$ ) (Riedel 1992; Haines et al. 2001). Often materials with high bulk moduli values are seen to possess high hardness values (Riedel 1992; Haines et al. 2001; Brazhkin 2007; Leger et al. 1994). This is based on the fact that such materials would resist deformation when subjected to high loads owing to their high stiffness values. However it is a source of substantial confusion that high bulk modulus and high hardness are discussed together and many a time omitting the contribution by the shear modulus. In reality there exists a better correlation, with reasonable scatter between hardness and shear modulus,  $G$ . Furthermore plastic deformation is initiated when the shear component of the applied stress exceeds the yield stress (Zerr and Riedel 2000). Thus the prediction of hardness values using the bulk moduli values alone may be misleading owing to this large scatter of the hardness-bulk modulus relationship. In view of this, these three main approaches have become the 'radar' to designing potential superhard materials. The first approach justifies the focus on the lighter elements boron, carbon, nitrogen and oxygen which form compounds with short covalent bonds. This has prompted research into three-dimensional boron-rich compounds (e.g.  $B_6O$ ,  $B_{22}O$ ,  $B_4C$ ,  $B_{25}N$  and  $B_{53}N$ ) (Riedel 1994), boroncarbonitrides ( $B_xC_yN_z$ ) (Badzian 1981; Nakano et al. 1994; Knittle et al. 1995; Nakano 1996; Zhao et al. 2002; Komatsu et al. 1996; Solozhenko et al. 2001; Mattesini and Matar 2001; Lambrecht and Segall 1993; Pan et al. 2005, 2006; Sun et al. 2001; Tateyama et al. 1997; Widany et al. 1998) and the hypothetical  $C_3N_4$  (Riedel 1994; Teter et al. 1996; Malkow 2001). On the other hand, the hardness values of existing superhard materials have been enhanced by manipulating the grain morphologies through various techniques. This second approach has led to a hybrid of nano-grained superhard materials with improved mechanical properties (Haines et al. 2001; Brazhkin 2007). The third approach focuses on achieving the goal through high bulk modulus elements. In this case the elements do not possess high enough hardness values to be considered 'superhard'. Compounds have been tailored by alloying with small, covalent bond-forming atoms such as boron, carbon, nitrogen and oxygen structures with high-packing indexes (Brazhkin 2007). This has led to another hybrid of highly incompressible hard materials such as  $RuO_2$  (Brazhkin 2007) WC and  $Co_6W_6C$  (Dubrovinskaia et al. 1999) transition metal borides ( $TiB_2$ ,  $WB_4$ ,  $WB_2$  and WB) and  $BeB_2$  (Brazhkin).

However despite the efforts, the first two approaches seem to have yielded materials with hardness values approaching that of diamond but not exceeding it. The progress in obtaining superhard materials using the third approach has somewhat been hindered by the fact that most of the compounds in this group possess some degree of ionicity (bonds not purely covalent) with low shear component values (Haines et al. 2001). Against this background, clearly it remains a challenge to experts in the materials science field to find substitute materials which fully complement diamond in this regard.

### **3 Influence of Microstructural Parameters on the Mechanical Properties**

It is apparent that the majority of macroscopic properties of polycrystalline materials are directly influenced by the microstructure. There are a number of microstructural parameters of importance each of which has a certain influence on the specific property in question. This section will highlight those parameters that should be considered, and more detail will be found in the subsequent sections looking at the specific properties. One of the most important factors in a given microstructure is the grain size, grain size distribution and grain shape. These have a direct influence on the hardness, fracture toughness, strength, wear and thermal properties as discussed in subsequent sections. The microstructure can therefore be tailored to suit certain needs depending on the targeted performance level. The grain size distribution in some instances gives an indication of the packing index of the particles which is quite important especially for liquid infiltrated compacts.

Another parameter of importance is the contiguity in composite materials especially in the case where there is significant contrast in properties, e.g. WC/Co and polycrystalline diamond compacts. This effectively indicates the different volume fractions of the phases present and has a direct influence on performance. Lastly, interface composition is also a very important feature which affects almost all the mechanical properties and can be controlled to target certain performance levels.

### **4 Establishing Structure-Property Correlations of Superhard Materials**

From the above discussion, it is a well-established fact that the mechanical characteristics of most materials depend on both microscopic properties (i.e. interatomic forces) and macroscopic properties (i.e. morphology, stress fields, defects, possible inhomogeneities, etc). As such it is imperative to establish a correlation between these properties with the behaviour of materials. In accordance with earlier

discussions, superhard materials can be classified into four groups as specified in the work of Brazhkin et al. (2002):

- (i) Compounds formed by light elements from periods 2 and 3 of the periodic table. These normally form covalent and ionic-covalent bonds.
- (ii) Crystalline and disordered carbon modifications with covalent bonds.
- (iii) Partially covalent compounds between transition metals and light elements, e.g. borides, nitrides, oxides and carbides.
- (iv) Nanostructured materials.

## 4.1 Group 1 Compounds

Typically superhard materials from this group are made from elements in the middle of period 2 and 3. These are capable of forming tight three-dimensional rigid lattices with short, non-polar covalent bonds. These bonds offer maximum resistance to atomic movement and are directional, and they would rather be broken than bent (Sung and Sung 1996). This includes compounds of boron, carbon, nitrogen and oxygen. The small atomic radii enable the formation of short interatomic distances and a high coordination number (C-N) (Sung and Sung 1996). This allows atoms to be surrounded by a large number of neighbours with a high degree of covalence. The combined effect is to basically concentrate the bond energy in a small volume thus a substantial amount of stress is required to deform such a crystal lattice (Sung and Sung 1996). Examples of compounds in this group include boron-rich compounds ( $B_6O$ ,  $B_{22}O$ ,  $B_4C$ ,  $B_{25}N$ ,  $B_{13}C_2$ , and  $B_{53}N$ ), boron carbonitrides  $B_xC_yN_z$  and the hypothetical  $C_3N_4$  (Brazhkin et al. 2002; Sung and Sung 1996; Kurakevych 2009).

Several modifications of boron compounds have been reported (Kurakevych 2009). The boron structure consists of an icosahedra  $B_{12}$  bonded with covalent bonds (Kurakevych 2009). Four allotropic modifications of boron have been reported, i.e. rhombohedral  $\alpha$ - $B_{12}$  (Decker and Kasper 1959), rhombohedral  $\beta$ - $B_{106}$  (Hughes et al. 1963), tetragonal  $\tau$  -  $B_{192}$  and orthorhombic  $\gamma$  -  $B_{28}$  (Oganov et al. 2009). Two-element boron phases have been synthesised which include cubic boron nitride (c-BN), second to diamond in hardness. Also some subnitrides have been reported, i.e.  $B_{50}N_2$ ,  $B_6N$ ,  $B_4N$  and  $B_{13}N_2$ , characterised by high hardness values due to the short covalent bonds they possess. Boron carbides are known to possess remarkably higher oxidation resistance and interaction with iron group metals than other carbon-based materials (Kurakevych 2009). The B-O system has generated boron suboxides (e.g.  $B_6O$ ) with typical hardness values close to that of superhard materials (~40 GPa). The C-N system still remains hypothetical with the  $C_3N_4$  cubic phase predicted to have shorter covalent bonds than diamond and hence harder than diamond. However experimental data has shown that  $C_3N_4$  is much less harder than diamond although the results are still debatable; this clearly indicates that hardness properties cannot be predicted from bond length alone (Brazhkin et al. 2002; Sung and Sung 1996; Kurakevych 2009).

## 4.2 Group 2: Carbon-Based Materials

This forms a special group of superhard materials due to the existence of a variety of chemical bonds between carbon atoms (Oganov et al. 2009). Diamond, the hardest material known to man to date, consists of  $sp^3$ -hybridised carbon bonds. Single crystals of diamond possess high values of elastic constants  $c_{11}$  and  $c_{44}$  as well as low Poisson's ratio  $\sim 0.07$  (Frantsevich 1980; Novikovin 1987; Kurdumova et al. 1984). Lonsdaleite is another  $sp^3$ -hybridised modification of carbon possessing similar mechanical properties to diamond. There are a number of  $sp^2$ -hybridised hypothetical carbon structures which have been investigated theoretically (Liu et al. 1981). These however possess lower bulk moduli values (50–370 GPa) than diamond (Brazhkin et al. 2002). Fullerenes form a family of  $sp^2$ -hybridised superhard phases with extremely high bulk moduli values (800–900 GPa), twice as high as that of diamond (Ruoff and Li 1995). A typical example includes the  $C_{60}$  molecule, a naturally soft molecular crystal, which tends to harden under very high pressures (50–70 GPa) (Brazhkin et al. 2002). Worth mentioning is the amorphous diamond-like hard carbon (DLHC). What governs the high hardness and strength values for these phases is basically the small carbon atom radii capable of forming short bonds coupled with four-coordinated non-polar directional covalent bonds similar to what was discussed in group 1 above (Fig. 3.2).

## 4.3 Group 3: Transition Metal Compounds

A number of transition metals possess high bulk moduli values but do not possess high enough hardness values to be considered *superhard*. In principle, the transition metals could introduce a high valence electron density to resist elastic deformation whereas the light metals can introduce short and strong covalent bonds with high resistance to slipping under stress. Superhard compounds have been tailored by alloying with small, covalent-forming atoms such as boron, carbon, nitrogen and oxygen to form structures with high-packing indexes (Brazhkin et al. 2002; Matizamhuka 2010). The leaders in this class are the borides, e.g.  $WB_4$ ,  $WB_2$  and  $WB$ , with approximate hardnesses of 36–40 GPa (Brazhkin et al. 2002). Other highly incompressible compounds have been reported in this group which include  $RuO_2$  (Leger et al. 1994),  $Co_6W_6C$  (Dubrovinskaia et al. 1999),  $BeB_2$  (Brazhkin et al. 2007),  $ReB_2$ ,  $OsB_2$ ,  $WB_4$ ,  $IrN_2$ ,  $PtN_2$  and  $TiB_2$  (Brazhkin et al. 2002; Veprek 2013); however carbides and nitrides are inferior in hardness to borides (Brazhkin et al. 2002). It should be noted that some of the compounds formed in this group are not purely covalent and in some instances possess some degree of ionicity thus limiting the hardness/strength properties.

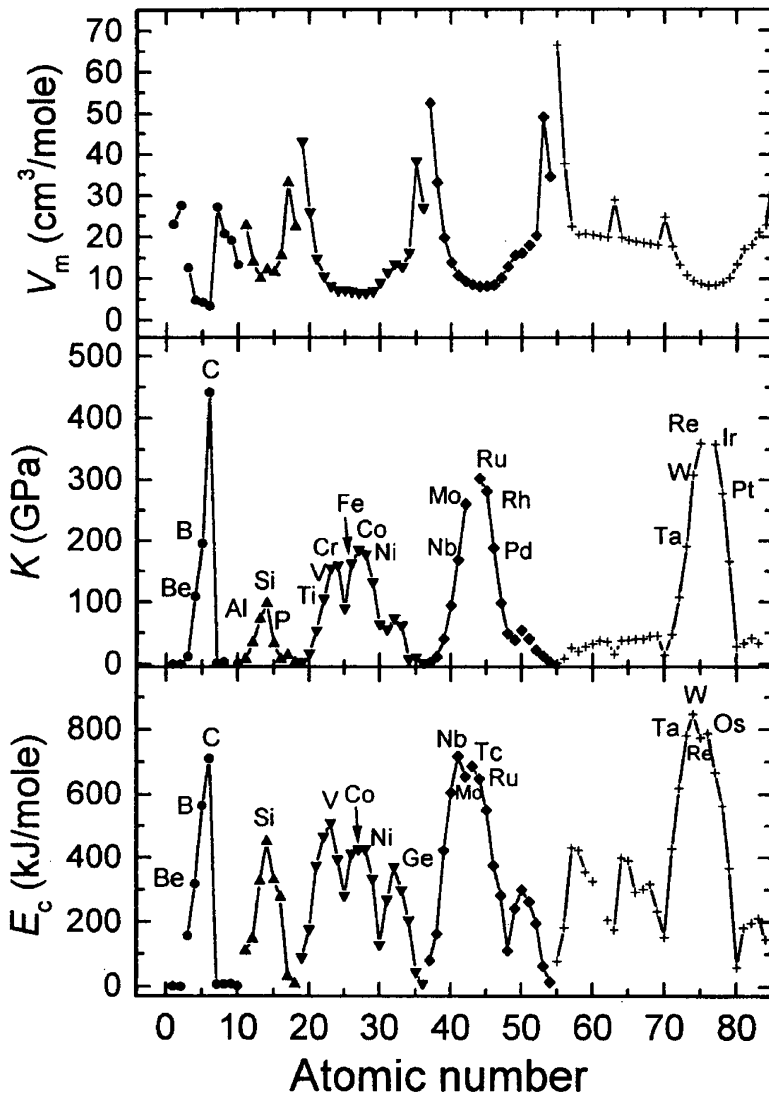


Fig. 3.2 Schematic representation of the dependency of certain physical properties on the atomic number, i.e. molar volume  $V_m$ , bulk modulus  $K$  and cohesive energy  $E_c$  (Brazhkin et al. 2002)

#### 4.4 Group 4: Nanocrystalline and Superlattice Structures

The above discussions highlight the possibility of obtaining superhard structures through microscopic property interactions. However limitations arise owing to deviations from ideality, e.g. non-uniform distribution of electron density may arise and distortion in the four-coordinated structure may also arise. This introduces



differences between the real and ideal hardnesses of most of the covalent compounds in the preceding groups. However, it is possible to reduce this difference by tailoring the morphology/inhomogeneity of these compounds (Brazhkin et al. 2002; Veprek 2013). There are two limiting cases in which the real hardness can be substantially improved:

- (i) In the ideal defect-free crystal where dislocations are absent
- (ii) In the amorphous or nanocrystalline state where there is maximum hindrance to dislocation motion

Obviously defect-free crystals cannot be easily obtained for several thermodynamic reasons (e.g. thermal activation of point defects) (Brazhkin et al. 2002). On the other hand, amorphous solids may contain some defects within the network which effectively introduce deviations from 'ideal' ordering of the amorphous networks thus introducing deviation from ideal hardness (Davis 1976; Mott and Davis 1979). It is clear from the practical standpoint that the properties of superhard materials can be enhanced through grain refinement into the nano-range. This is discussed in much further details in Chap. 6.

In a number of cases, the practically achievable mechanical properties of most engineering materials are orders of magnitude lower than theoretical ones owing to the presence of flaws/defects in structures. Most of these defects (e.g. dislocations, microcracks, grain boundaries) are quite prone to shearing and can easily grow under stresses much lower than the ideal strength, thus limiting the material strength and hardness values (Veprek 2013). By reducing the grain size, the flaw/defect size is decimated which in turn strengthens grain boundaries by hindering dislocation multiplication and motion (Liu and Cohen 1989). Traditionally strengthening of materials has been achieved by well-known metallurgical principles such as solution hardening, work hardening and grain boundary hardening (Veprek 1999; Hertzberg 1989; Kelly and MacMillan 1986; Inoue et al. 1994). It must be noted that solution and work hardening do not operate in small nanocrystals of  $\leq 10$  nm due to solute atoms segregating at grain boundaries where there are no dislocations (Veprek 1999). Thus the grain boundary hardening concept would be more relevant to superhard materials. To get a more in-depth understanding of the property-size effect, a look into the Hall-Petch relation is vital at this point. The Hall-Petch relation correlates the material's ideal properties (hardness, strength, critical fracture stress) to the crystallite size. This relation has traditionally been used to explain the strengthening effect of a wide range of materials as a function of crystallite/grain size. Thus the Hall-Petch relation can be rewritten as follows:

$$\sigma_c = \sigma_0 + \frac{k_{gb}}{\sqrt{d}} \quad (3.1)$$

Here  $\sigma_c$  is the critical fracture stress,  $d$  the crystallite size and  $\sigma_0$  and  $k_{gb}$  are constants. However at smaller crystallite sizes, i.e. below 10 nm, reverse Hall-Petch dependence occurs due to various mechanisms described and reviewed in Refs (Veprek 1999; Veprek and Argon 2001; Ashby 1972; Luthy et al. 1979;

Mohamed and Langdon 1974; Crampon and Escaig 1980) and also later on in Chap. 6. Computer simulation studies have shown that the reverse Hall-Petch dependence in nanocrystalline metals is due to the grain boundary sliding as a result of small sliding events of atomic plains at the grain boundary without thermal activation (Veprek 1999; Schiotz et al. 1998). In principle, a further increase in strength and hardness with decreasing grain size can be achieved by blocking grain boundary sliding (grain boundary hardening) (Veprek 1999). Grain boundary hardening can be affected by the use of nanocrystalline/amorphous grain boundary filler as suggested by Veprek (1999). It is important that such nano-phases should be refractory and stable at high temperatures and possess high structural flexibility in order to accommodate coherency strain without forming dangling bonds (discontinuity), voids or other flaws (Veprek 1999).

Alternatively, the relation can be understood through the general Griffith formula relating the critical stress causing growth of microcracks of size to the flaw size  $a_0$ :

$$\sigma_c = k_{\text{crack}} \sqrt{\frac{2E\gamma_s}{\pi a_0}} \propto \frac{1}{\sqrt{d}} \quad (3.2)$$

Here  $E$  is the Young's modulus,  $\gamma_s$  is the surface cohesive energy and  $k_{\text{crack}}$  is a constant dependent on the nature and shape of the microcrack and type of stress applied. In principle, the flaw size  $a_0$  in a well-compacted material is always smaller than the crystallite size, i.e.  $a_0 \leq d$  (Veprek 1999). Thus a reduction in grain size will effectively reduce the size of flaws and at much smaller sizes will in turn decimate or even eliminate most flaws. This is further discussed in Chap. 5 which looks at fracture toughness, methods of measuring it and their limitations.

Another design concept is depositing epitaxial multilayers having different elastic constants but similar thermal expansion and strong bonds as proposed by Koehler (1970). These multilayers are referred to as heterostructures or superlattices (Veprek 1999). Superhard epitaxial nano-polycrystalline superlattices of nitrides and oxides have been reported, e.g. TiN/VN (Helmersson 1987) and TiN/NbN (Shinn et al. 1992; Chu et al. 1992; Larsson et al. 1996). A hardness increase by a factor of 2–4 was achieved when the lattice period decreased to about 5–7 nm, e.g. for TiN/NbN a hardness of ~50 GPa was reported with a lattice period of 4 nm (Shinn et al. 1992). The question here is 'What really makes superlattices superhard?' If one considers the separate layers making up superlattices, they possess hardnesses lower than 40 GPa, but in the combined state, there is substantial enhancement of hardness values to reach or even exceed 40 GPa. This can be explained by how effective these structures are capable of hindering dislocation motion. Normally, the thicknesses of these layers are kept small to avoid dislocation operating within the layers (Veprek 1999). Under an applied stress, a dislocation may form in the softer layer, and as it moves towards the interface, elastic strain induced in the second layer (with higher elastic modulus) would case a repulsing force that would hinder dislocation from crossing the interface (Veprek 1999). This

basically enhances the strength/hardness of the layers. For further reading on the theories of superlattice properties, the reader is referred to the reviews by Barnett (1993) and Anderson and Li (1995). At this point it would be appropriate to introduce the most prominent mechanical properties of superhard materials and relate them to the respective structures. The word ‘most prominent’ is used here to highlight the properties that we are putting more emphasis on. What really qualifies most of the superhard materials in most of the industrial applications is their ability to withstand extreme conditions during, for example, cutting applications. Here high hardness, good wear, fracture toughness and thermal properties are most important. Thus what follows below is an insight into the relations between these specific properties with the material properties.

## 5 The Hardness Paradigm

Hardness can be defined as the resistance of a material to elastic and plastic deformation (Veprek 1999, 2013). This deformation begins when the shear component of the applied stress exceeds the yield stress (Matizanhuka 2010; Veprek 1999, 2013; Davis 1976; Mott and Davis 1979; Liu and Cohen 1989). Hardness is strongly influenced by residual stresses, toughening phases, microstructural textures, grain size, applied load, porosity and structure and composition of grain boundaries (Veprek 1999, 2013; Cottrell 1967). The hardness value is given by a ratio of the applied load to the area of surface contact of a hard indenter, usually diamond, loaded perpendicular to a planar surface of the material under test. The measured hardness value of any material depends on parameters associated with the test method and indenter geometry (Matizanhuka 2010; Veprek 1999, 2013; Cottrell 1967). It varies with the applied load, indenter shape and dimensions, microstructure and prior history of the material, loading rate, the environment and the test temperature (Matizanhuka 2010; Veprek 1999, 2013; Cottrell 1967). Thus in order to compare hardness values of different materials, the specific test method and test conditions have to be described carefully (Matizanhuka 2010; Veprek 1999, 2013; Cottrell 1967).

Theoretical attempts to describe hardness in terms of the elastic bulk or shear moduli of an ideal solid are not uncommon. The elastic moduli are an intrinsic mechanical property of a material dominated by the strength of the chemical bonds between the atoms (Matizanhuka 2010; Veprek 1999, 2013; Cottrell 1967). The high elastic moduli of superhard materials reflect the strong chemical bonds between the atoms. These bonds are predominately covalent in nature. In general, ionic/covalent bonds deform less than metallic bonds under a given external force (Matizanhuka 2010; Veprek 1999, 2013; Cottrell 1967). Thus the theoretical hardness assumes higher values at greater elastic moduli values. This ‘theoretical’ hardness is proportional to the reciprocal value of the bulk modulus,  $B$  (Matizanhuka 2010; Veprek 1999, 2013; Cottrell 1967).

There is a relationship between the bulk modulus  $B$ , the applied stress  $\psi$  and  $\epsilon$  the elastic strain from Hooke's law,

$$B = \frac{d\psi}{d\epsilon} \quad (3.3)$$

and from the binding energy  $E_b$ , bond length and stress relation,

$$\psi = \frac{dE_b}{da} \quad (3.4)$$

Clearly there is a direct relationship between the bulk modulus,  $B$ , and the binding energy,  $E_b$ , and the interatomic bond distance,  $a$ , which is described by the equation below:

$$B = \frac{d^2E_b}{da^2} \quad (3.5)$$

Thus high bond energy means high electron density between the atoms as in non-polar covalent bonds formed between atoms of small radii of the first period which explains the high hardness values attained by compounds of these elements (Matizanhuka 2010; Veprek 1999, 2013). A more common bulk modulus-bond length relationship which has been used to predict the theoretical hardness values of most existing and potential superhard materials is given by the equation below (Matizanhuka 2010; Veprek 1999, 2013; Cottrell 1967):

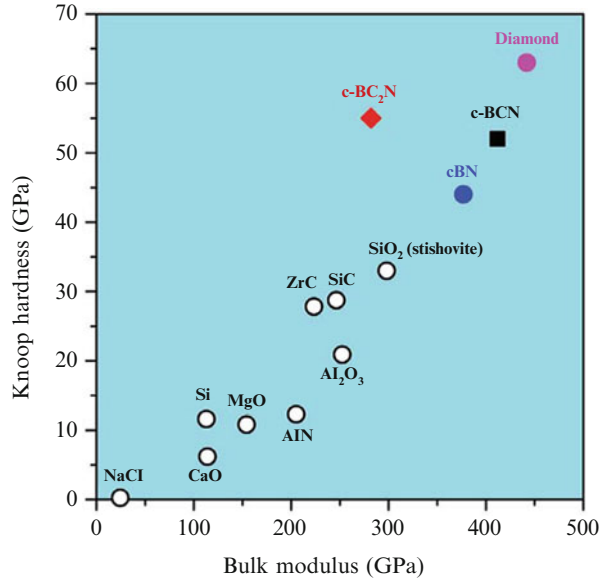
$$B(GPa) = \left(\frac{N_c}{4}\right) \left(\frac{1971 - 220\lambda}{d^{3.5}}\right) \quad (3.6)$$

where,  $N_c$  is the coordination number,  $d$  is the bond length ( $\text{\AA}$ ) and  $\lambda$  is an empirical parameter measuring the polarity of the bond. For non-polar covalent bonds such as in diamond,  $\lambda = 0$ , in other compounds such as c-BN,  $\text{Si}_3\text{N}_4$  and SiC,  $\lambda > 0$ , hence the lower bulk moduli and hardness values for these compounds compared to diamond (Fig. 3.3).

Clearly, a high coordination number is required in order to maximise the value of  $B$ . Also a high bond energy as found for non-polar covalent bond between atoms of small radii results in high theoretical hardness. This explains the reason why carbon in its metastable fourfold-coordinated  $\text{sp}^3$  hybridisation in diamond forms the hardest known material followed by c-BN. Also the expected high theoretical hardness of  $\text{C}_3\text{N}_4$  is based on this prediction, i.e. a small C-N bond distance and relatively small polarity.

However it has been argued that materials deform plastically only when subjected to a shear stress (Cottrell 1967). Thus the shear stress needed for dislocation motion and multiplication to cause plastic deformation is proportional to the elastic shear stress of a deformed material (Cottrell 1967). Thus the

**Fig. 3.3** A schematic representation of the Knoop hardness as a function of bulk modulus of some hard and superhard materials (Solozhenko and Gregoryanz 2005)



prediction of hardness using the bulk modulus value may be misleading owing to the greater scatter of hardness-bulk modulus relationship. Gilman (1973) and Liu and Cohen (1989) established a linear correlation between hardness and bulk modulus. This was subsequently followed by an improved correlation between hardness and shear modulus proposed by Teter and Hemeley (1996). Most pre-2012 publications have been based on these empirical correlations to predict the hardness of potential/new superhard materials (Tian 2012). In recent years, the use of these simple linear correlations has increasingly become questionable. This is due to the fact that the bulk modulus which is a measure of a material incompressibility depends largely on the valence electron density. Thus the greater the electrons involved, the greater the repulsions within a structure implying a higher value of  $B$ . On the other hand, the shear modulus which measures the resistance to shape change at a constant volume gives an indication of the material's ability to resist shearing forces. Clearly, both bulk and shear moduli are elastic in nature and correspond to reversible elastic deformation. It should be noted that with hardness, a permanent plastic deformation occurs, and this basically makes the predictions made earlier by Cohen and Gilman unreliable for predicting the hardness values of materials.

A more reliable relationship was proposed by Chen et al. (2011) which incorporates both the elastic and plastic properties of pure polycrystalline metals. Chen et al. proposed a ratio referred to as the Pugh's modulus ratio  $k = G/B$  which relates the brittleness,  $G$ , to the ductility  $B$  of materials. Thus brittle materials are bound to possess a larger  $k$  value compared to ductile ones. The Pugh's ratio is related to the Vickers hardness,  $H_V$ , through the correlation:

$$H_V = 2(k^2G)^{0.585} - 3 \quad (3.7)$$

This agrees well with experimental data.  $G/B$  depends monotonically on Poisson's ratio according to the relationship:

$$\nu = \frac{(3 - 2\frac{G}{B})}{(6 + 2\frac{G}{K})} \quad (3.8)$$

The Poisson's ratio correlates the bond stiffness and hardness of a material. It formally takes values between  $-1$  and  $0.5$ ; thus the lower limit generally corresponds to a material that does not change its shape and the upper limit to the unchanged volume (Brazhkin et al. 2002). For systems with predominantly ionic and van der Waals-type bonds,  $\nu$  is close to  $0.25$  corresponding to  $G/B = 0.6$ . For metallic structures  $\nu$  lies between  $0.3$  and  $0.4$  with  $G/B$  in the range  $0.2 < G/B < 0.5$ . Most covalent compounds  $\nu < 0.25$  and  $G/B > 0.6$ . Very few covalent compounds have a shear modulus exceeding the bulk modulus,  $G > B$  ( $\nu < 0.125$ ) (Brazhkin et al. 2002). The only such compounds include diamond, c-BN, quartz ( $\alpha$ -SiO<sub>2</sub>), lonsdaleite, B<sub>6</sub>O, HfB<sub>2</sub>, ZrB<sub>2</sub> and TiB<sub>2</sub> (Brazhkin et al. 2002). The high  $G/B$  ratios in most covalent compounds are associated with high angular stiffness of directional covalent bonds (Brazhkin et al. 2002). This stiffness plays quite an important role especially when coordination decreases from four towards lower values (Brazhkin et al. 2002). At higher coordination numbers ( $>4$ ), there is normally loss of directionality in covalent compounds and hence decrease in bond-bending forces (Brazhkin et al. 2002).

These predictions are based on macroscopic concepts which make it difficult to relate hardness to the microstructure of a material (Tian 2012). To understand the fundamental parameters controlling hardness, one needs to find a correlation between hardness and microscopic parameters (Tian 2012). In principle, at microscopic level, hardness measures the combined resistance of chemical bonds to indentation (Tian 2012). This implies that the greater the number of bonds in a region of the surface, the harder the material. Thus, it would be scientifically correct to correlate hardness to bond resistance, bond strength and electronegativity of a material. This simply implies that harder crystals are characterised by short and strong chemical bonds, high valence electron density/ high bond density and strongly directional bonds.

Another important aspect that plays a crucial role in hardness enhancement is grain refinement into the nano-range as described in the above sections. Conventionally, the enhancement can be explained through the hardening effect of grain boundaries as expressed by the Hall-Petch equation:

$$H = H_0 + \frac{k_{HP}}{\sqrt{D}} \quad (3.9)$$

Here  $K_{HP}$  is Hall-Petch hardening coefficient (sample dependant),  $D$  grain size (nm) and  $H_0$  hardness of bulk single crystal.

This concept is based on the fact that reducing crystallite size results in strengthening and hardening due to a more effective impediment of plasticity by the increased number of grain boundaries (Veprek 2013). However, this has been observed to be limited to a crystallite size down to 10–15 nm, and below this range, softening arises as grain boundary shear dominates (Veprek 1999, 2013). The reader can also refer to Chap. 6 where this is discussed in greater detail. It is interesting to note that larger enhancement of the hardness can be achieved even at finer crystallite size (3–4 nm) if low energy grain boundary or a strong interfacial layer is formed. At finer crystallite sizes, the number of defects decreases such as dislocations, twins, microcracks and others. These defects easily shear and grow upon a stress much lower than the ideal strength thus limiting the strength and hardness values (Veprek 1999, 2013).

Macrohardness testing of ceramic materials normally results in considerable cracking which may disguise the corners of the impression (Matizanhuka 2010; Veprek 1999, 2013). The extent of cracking is related to grain size and fracture toughness, and acceptable measurements are feasible below 5 kg in most cases (Matizanhuka 2010; Veprek 1999, 2013). Recommended practice is that a quoted number for a material should be the average from 5 to 10 randomly positioned macrohardness tests and preferably more than 20 randomly positioned microhardness tests (Matizanhuka 2010; Veprek 1999, 2013). This is done owing to the scatter of results normally obtained on ceramics as a result of their multiphase nature, their generally non-cubic symmetry and porosity that exists below the surface of the test piece (Matizanhuka 2010; Veprek 1999, 2013). It is therefore not uncommon to obtain coefficients of variation of 10 % in macrohardness measurements and 20 % in microhardness measurements (Matizanhuka 2010; Veprek 1999, 2013). Chapter 4 discusses the various techniques for hardness measurements and their limitations. The chapter also proposes ways in which such difficulties can be overcome in order to obtain accurate values of hardness.

## 5.1 Factors Affecting Hardness

The hardness of brittle materials has a strong dependence on the flaws present which act as stress concentration sites incapable of relaxing plastic deformation (Teter and Hemeley 1996). These flaws are present in many forms in most hard materials, the most prominent being residual stresses, microstructural textures, grain size, porosity and the structure of grain boundaries (Evans and Lange 1975). In practice sintered specimens usually have a relative density below 99 % (Evans and Lange 1975). This leaves some residual porosity which has been found to affect the hardness in a negative sense (Evans and Lange 1975). Pores are less resistant to indent penetration thus they present regions of low hardness in the material. It has been observed that small porosity levels of 1–2 % can affect the hardness more than an increase in the grain size from 0.5  $\mu\text{m}$  to 2  $\mu\text{m}$  (Evans and Lange 1975).

It has been observed that any polycrystal exhibits a hardness like the single crystal if the load is small enough, i.e. if only a few grains are affected (Evans and Lange 1975). At higher loads the indentation size becomes much larger than the grains, and in polycrystals, this size effect is partly offset by the hindrance of dislocation activity due to close spacing of grain boundaries, in the case of fine-grained microstructures (Evans and Lange 1975). On the other hand, with coarse-grained microstructures, there is less resistance to plastic deformation because of lower hindrance to dislocation activity. This in itself explains why fine-grained materials are found to be harder than their coarse-grained counterparts. This is also highlighted in the Hall-Petch relationship which shows an inverse relationship between the hardness and the grain diameter,  $d$  (Evans and Lange 1975).

Hardness has also been found to be affected by the structure of grain boundaries typically in liquid-phase sintered materials (Brazhkin et al. 2004). Theoretically  $\text{Si}_3\text{N}_4$  has a Vickers hardness in the region of  $\sim 17\text{--}18$  GPa, but the liquid-phase sintered counterpart has a reduced hardness (Brazhkin et al. 2004). This reduction in hardness is thought to be due to lowered resistance to indent penetration by the binder material present at the grain boundaries.

The factors discussed above are all related to the material properties. There are also factors related to the environment such as temperature and moisture present and those related to the equipment used such as geometry of the indent and magnitude of the applied load. Detailed discussions of these factors are dealt with thoroughly in various other publications (Brazhkin et al. 2004; Lawn et al. 1975).

## 6 Fracture Mechanics of Superhard Materials

Superhard components in most cases fail by unstable propagation of cracks initiated at flaws which are present due to manufacture or surface treatment (Evans and Lange 1975). These flaws are usually in the form of pores, cracks and inclusions. The brittle behaviour of superhard materials is attributed to low resistance to crack propagation (Brazhkin et al. 2004; Lawn et al. 1975). There are two main methods used for characterising the crack propagation behaviour of materials. The more commonly used method is the evaluation of the fracture toughness  $K_{IC}$ .  $K_{IC}$  is a critical value of the stress intensity factor  $K_I$ . The latter quantity serves as a scale factor to define the magnitude of the crack tip stress field (Lawn et al. 1975).  $K_I$  is dependent on the applied load, initial size of crack and geometry of the component (Lawn et al. 1975) and has been found to increase until unstable crack propagation occurs at some critical value, i.e.  $K_I = K_{IC}$  (Niihara et al. 1982). There are basically three loading modes which result in high stresses at the crack tip, namely:

- (i) Mode 1: tension normal to the crack plane
- (ii) Mode 2: shear loading in crack direction
- (iii) Mode 3: out of plane shear loading

Mode 1 has been found to be the most important (Niihara et al. 1982).



An alternative method is based on energy considerations in crack propagation described by the crack resistance factor  $G_{IC}$ . This idea is referred to as the Griffith criterion (Lawn et al. 1975; Niihara et al. 1982). The criterion compares the magnitude of the strain energy released to that consumed by a crack increment, the so-called  $R$ , representing the resistance to cracking (Niihara et al. 1982). An equilibrium condition occurs when the difference,  $G-R = 0$ , and crack growth is favoured if  $G-R > 0$  and healed when  $G-R < 0$ . This forms the basis of the Griffith criterion (Niihara et al. 1982).

It has been observed that the most problematic part of toughness determination is to create a crack and to measure its size (Lawn et al. 1975). There are several methods in use for fracture toughness determination, detailed discussion of which is presented in a number of publications (Evans and Lange 1975; Brazhkin et al. 2004; Lawn et al. 1975; Niihara et al. 1982) and in Chap. 5.

### 6.1 Vickers Indentation Cracks

Fracture toughness determination with Vickers hardness indentations was proposed by Evans et al. (1976) and later extended by Niihara et al. (1982) and Anstis et al. (1981). The fracture toughness is calculated from the length of cracks which develop during a Vickers indentation test and can be measured optically at the specimen surface (Niihara et al. 1982; Evans and Charles 1976; Anstis et al. 1981). The basic procedure for fracture toughness determination consists of three main steps, namely (Brazhkin et al. 2004):

- (i) Generation of a crack in a test specimen
- (ii) Measurement of load of failure
- (iii) Calculation of  $K_{IC}$  from failure load, failure stress and crack depth using relations dependent on crack length, specimen dimensions and yield stress

The fracture toughness value can be obtained from the relation (3.10):

$$K_{IC} = 0.032H\sqrt{a}\left(\frac{E}{H}\right)^{\frac{1}{2}}\left(\frac{c}{a}\right)^{-\frac{3}{2}} \quad (3.10)$$

$H$  is the hardness,  $E$  is the Young's modulus,  $a$  is half the indent diagonal and  $c$  is the length of crack (Brazhkin et al. 2004).

In the development of new superhard or composite materials, the Young's modulus value,  $E$ , is usually unknown. It is common practice to adopt relations independent of  $E$ ; Shetty et al. (1981) developed a relationship based on the Palmqvist radial cracks found on the specimen surface shown below (Anstis et al. 1981; Shetty et al. 1985):

$$K_{IC} = 0.0889 \sqrt{\left(\frac{H \times P}{4l}\right)} \quad (3.11)$$

$H$  is the Vickers hardness,  $P$  is the indent load,  $l = c - a$  where  $2a$  is the indent diagonal and  $2c$  is the length of full crack.

The development of cracks in brittle materials occurs in a sequence of steps. Under the indentation load, the elastic limits of most ceramic materials are exceeded, and a zone of plastic deformation develops beneath the pyramidal indenter (Evans 1974a, b; Munz and Fett 1999; Olagnon et al. 2006; Elssner et al. 1999). The indenter acts as a wedge and induces tensile stresses in the surrounding material (Evans 1974; Munz and Fett 1999; Olagnon et al. 2006; Elssner et al. 1999). During the loading phase, these tensile stresses overlap with compressive stresses caused by the applied indentation load. There is development of cracks but with restricted mobility. When the load is removed from the indenter, the compressive stress component ceases to exist, and cracks formed assume their final length (Evans 1974a, b; Munz and Fett 1999; Olagnon et al. 2006; Elssner et al. 1999). The cracks will grow to a point at which the stress intensity falls below its critical value (Evans 1974a, b; Munz and Fett 1999; Olagnon et al. 2006; Elssner et al. 1999).

Given the variety of cracking mechanisms associated with ceramic materials, both the stress field underload and the residual stress are clearly very complex (Evans 1974; Munz and Fett 1999; Olagnon et al. 2006; Elssner et al. 1999). Additionally in materials with large grain size and single crystals, irregular cracks and lateral cracks which proceed parallel to the surface causing chipping may develop (Evans 1974; Munz and Fett 1999; Olagnon et al. 2006; Elssner et al. 1999). The presence of residual stresses in the vicinity of the crack also results in subcritical crack growth in air. All these lead to an underestimation of the fracture toughness value. It is common practice to create indentation cracks in oil to avert subcritical crack growth in air and to measure the crack size immediately after indentation (Evans 1974; Munz and Fett 1999; Olagnon et al. 2006; Elssner et al. 1999).

## ***6.2 Influence of Microstructural Parameters on Toughening***

To improve the fracture toughness of superhard materials, it is imperative to accurately analyse the failure mechanisms and the structure-property relationship between fracture initiation and microstructure (Evans 1974). Over the years, the enhancement of toughness properties of advanced materials has been achieved by tailoring their microstructures to provide toughening mechanisms. In principle, toughening mechanisms can be categorised into two types: intrinsic and extrinsic. Intrinsic mechanisms operate ahead of a crack tip and are primarily related to plasticity, i.e. enlargement of the plastic zone which is effective against both

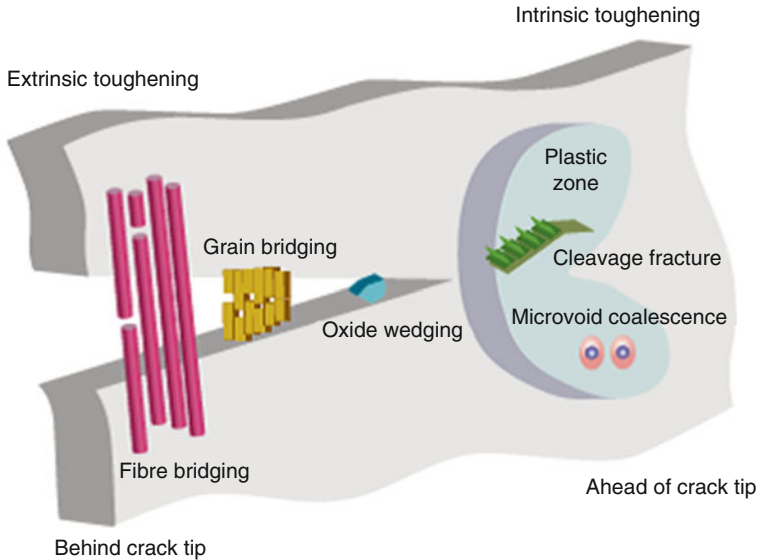


**Fig. 3.4** Schematic representation of extrinsic and intrinsic toughening mechanisms (Ritchie 2011)

crack initiation and propagation (Mcnamara et al. 2015; Zhu et al. 2015; Ritchie 2011; Krstic 1988). This is the primary source of toughening in ductile materials and is ineffective with brittle materials (Mcnamara et al. 2015; Zhu et al. 2015; Ritchie 2011; Gomez and Elices 2006; Krstic 1988). Conversely, extrinsic toughening acts primarily on the wake of the crack to shield local stresses and strains at the crack tip (Ritchie 2011). Effectively extrinsic toughening is usually associated with processes behind a crack tip<sup>2</sup>, and there has to be a crack for them to operate; thus they have no effect on crack initiation (Ritchie 2011). There are a variety of microstructural mechanisms utilised to effect extrinsic toughening which include crack bridging by unbroken fibres or ductile phase in composites, friction interlocking of grains during intergranular fracture in monolithic ceramics, meandering and crack surface sliding and shielding and microcracking in transformation-toughened ceramics (Launey 2009) (Fig. 3.4).

A classic example is the use of nanoscale glassy films along grain boundaries to promote boundary cracking and grain bridging in SiC. The fracture toughness of SiC is  $\sim 2\text{--}3 \text{ MPam}^{1/2}$  when it fractures transgranularly and can approach  $10 \text{ MPam}^{1/2}$  for intergranular fracture (Ritchie 2008, 2011). This is attributed to the greater crack-stopping power when the crack has to negotiate round the grains as opposed to propagating through the grains.

<sup>2</sup> Extrinsic toughening can also be caused by crack shielding, crack deflection from hard particles or along weak interfaces and crack branching as shown in the Appendix Fig. A1.

As discussed above the most important toughening mechanisms in polycrystalline brittle materials are the extrinsic type such as grain bridging and transformation toughening. It is thus imperative to understand how microstructural features affect the effectiveness of these mechanisms during design of new or prediction of toughness properties of old superhard materials. In grain bridging, frictional bridging occurs behind the crack tip when a reinforcement-matrix interface debonds and the reinforcement is further pulled out. This effectively acts to reduce the crack opening and provides a shielding effect. Thus the shielding effect depends on the reinforcement strength, volume fraction, size, the Young's modulus and the interface properties (Fantozzi and Saadaoui 2014). The relation between bridging stress,  $\sigma_b$ , and crack opening displacement,  $\delta$ , has been modelled and the more dominant bridging stress can be expressed as: (Launey et al. 2010)

$$\sigma_b = \sigma_m \left( 1 - \frac{\delta}{\delta_c} \right)^n \quad (3.12)$$

Here  $\sigma_m$  is the bridging stress,  $\delta_c$  is the crack opening displacement at which grain bridging disappears and the exponent  $n$  describes the stress decrease.

In view of the above, it is apparent that the magnitude of grain bridging is a function of the expansion anisotropy, interfacial roughness, grain size and morphology (aspect ratio), which can be controlled by additives or heat treatments (Fantozzi and Saadaoui 2014). Thus grain coarsening and elongating the microstructure enhances the frictional bridging and pull-out resulting in greater stress intensity factor (Fantozzi and Saadaoui 2014). Classical examples include coarse grain alumina and the so-called self-reinforced  $\text{Si}_3\text{N}_4$  (Fantozzi and Saadaoui 2014). It must be noted however that there exists a critical grain size above which a low intensity factor is observed due to appearance of transgranular fracture which reduces the grain-bridging effect (Fantozzi and Saadaoui 2014). In a recent study on leached polycrystalline diamond (PCD) compacts, the effect of a decreasing grain size shows a decrease in fracture toughness (Mcnamara et al. 2015). In principle, the finer the grain sizes have lower aspect ratios between adjacent grains thus presenting lower resistance to crack propagation compared to a coarse grain. In the case of a coarse grain size, a propagating crack will experience more resistance as it must negotiate around larger grains, thus increasing the energy required for fracture over the entire process. Transformation toughening is synonymous with  $\text{ZrO}_2$ -based ceramics. This occurs as a result a volumetric increase (~5 %) accompanying transformation which creates compressive stresses that shield the crack tip from the applied stress (Fantozzi and Saadaoui 2014; Launey et al. 2010; Nalla et al. 2003; Weiner and Wagner 1998). In essence, the magnitude of transformation toughening is controlled by the stability of the transforming phase which is influenced by the microstructure, i.e. grain size, morphology and location (along grain boundaries or inside the grains) ((Fantozzi and Saadaoui 2014)).

## 7 Strength of Brittle Materials

In principle the strength of a brittle material is not an intrinsic material property but more of a *conditional* property quite useful for design and comparison/ranking purposes (Kelly 1995). Thus strength values are strongly dependent on the material microstructure, processing history, testing methodology and environment and failure mechanisms. Griffith et al. (1920) pioneered the work on the strength behaviour of brittle materials using glass. He showed that strength is sensitive to microcrack-like defects and drew up a relationship between the fracture strength and flaw size.

In principle, Griffith showed that crack extension occurs in brittle materials when the stored elastic energy (mechanical energy) released during extension just exceeds the energy required to form new surfaces (surface energy) (Lawn et al. 1994). Under equilibrium conditions, we have the famous Griffith strength equation where the total system's internal energy (mechanical + surface energy) is unchanged with incremental crack extension (Kelly 1995; Griffith 1920; Lawn et al. 1994):

$$\sigma_f = \left( \frac{2E'\gamma}{\pi a_0} \right)^{1/2} \quad (3.13)$$

Here  $\sigma_f$  is the fracture strength in uniform tension,  $E'$  is the plain structure elastic modulus,  $\gamma$  is the surface energy per unit area and  $a_0$  is the starter flaw/crack size.

The classical Griffith relation links the material strength and toughness to a critical flaw size (Griffith 1921). Over the years a number of authors have demonstrated the relationship of the critical length scale to the material grain size in the presence of thermoelastic stresses (Mcnamara et al. 2015; Evans 1974; Krstic 1984). However in most of these analyses, the critical grain size was often not equal to the actual grain size (Manamara et al. 2015). A number of researchers have investigated the effect of a microstructure on the experimentally measured fracture toughness (Mcnamara et al. 2015; Taylor 1996, 1999, 2004, 2006; Taylor et al. 2005). They have demonstrated that for a number of engineering materials, the characteristic length scale can be related back to the microstructure. This is known as the *theory of critical distances (TCD)*. In principle, this theory uses the characteristic material length to predict the fracture toughness for notched specimen (Mcnamara et al. 2015).

From a conceptual point of view, the theory predicts that once an effective stress ( $\sigma_{eff}$ ) is reached across a grain length, that grain will fail and a crack will grow (Mcnamara et al. 2015). The TCD theory demonstrates that failure occurs when a distance-dependent effective stress exceeds the ultimate tensile strength/flexural strength,  $\sigma_0$  of a material (Mcnamara et al. 2015). The effective stress can be determined by a number of methodologies which include point method (PM), line method (LM) and area method (AM) which all use a characteristic length parameter calculated as follows (Mcnamara et al. 2015):

$$L = \frac{1}{\pi} \left( \frac{K_{IC}}{\sigma_0} \right)^2 \quad (3.14)$$

Here  $\sigma_0$  is the characteristic material strength. The most widely used methodologies are the LM and PM. The LM postulates that a material reaches its failure limit when the stress averaged over a line, starting from the notch equals the inherent material strength  $\sigma_0$  (Mcnamara et al. 2015).

In practice, the critical distance  $r_c$  is taken as the smallest microstructural feature and in the case of brittle polycrystalline materials is taken as the nominal grain size (Mcnamara et al. 2015). It must be noted that there exist errors associated with this whole approach; the reader is referred to references in McNamara et al. 2015 and the references therein for further reading (Mcnamara et al. 2015). This is also discussed in Chap. 5 as the authors evaluate the commonly used fracture measurement methods and their limitations when applied to hard, superhard and ultrahard materials.

## 7.1 Factors Affecting Strength

In practice most of the strength-controlling defects are introduced into materials during processing. These include porosity regions, agglomerates, inclusions and large-grained zones (Kelly 1995; Lange 1984). Furthermore, surface flaws are introduced by machining and grinding operations a material may be subjected to. Such defects act as weakness points/stress concentration sites yielding a range of ‘strength values’ for a given material. Secondly many practical aspects of testing can alter strength results which include specimen size effects, stress concentrations and failure mode (failure location, flaw type) (Kelly 1995). For instance, some materials will show lower strength when tested under humid or in the presence of moisture due to slow crack growth rate (Kelly 1995). Creyke et al. 1982 showed that strength is exponentially sensitive to slow crack growth parameter  $n$  by comparing time to failure ( $t_1, t_2$ ) under different static stresses ( $\sigma_1, \sigma_2$ ):

$$\left( \frac{t_1}{t_2} \right) = \left( \frac{\sigma_1}{\sigma_2} \right)^n \quad (3.15)$$

Although ASTM testing standards exist, there are problems that arise during testing that can produce inaccurate results such as alignment problems between specimen and test fixtures, specimen to support ratio dimensions, processing flaws and specimen thickness. In essence, strength values give an indication of the stress a specific material will support for a given flaw size distribution and failure mode (Kelly 1995). There are however complications that arise in determining strength values which are associated with the material structure, flaw size distribution and

failure mode. A widely accepted model for material and structural evaluation is the Weibull risk-of-rapture analysis given by the probability of failure below:

$$P_f = 1 - \exp\left\{-\frac{(\sigma - \sigma_n)^m}{\sigma_0}\right\} \quad (3.16)$$

Here  $\sigma_0$  represents a location parameter of Weibull distribution strength at 63.2 % failure probability (mean value in the Weibull normal distribution), and  $\sigma_n$  is the minimum strength and normally taken as zero. Note the exponent expression, which is evaluated over either a surface/volume from which failure can originate. An important assumption is that failure is a result of a single ‘failure type’ (structural inhomogeneity) (Frischholz 2004). In principle the Weibull modulus ( $m$ ) is a direct measure of the distribution of strengths. Thus the higher the Weibull modulus means the more uniform defects distribution and the more consistent the material. Put differently the material behaviour will be more consistent and the probability curve is narrower. Typical values in the range  $10 < m < 20$  have been achieved using four-point bending method (Frischholz 2004). It must be noted here that since the number of defects is dependent on the sample volume, the strength of larger parts is normally less than what is measured on the sample (Frischholz 2004).

## 7.2 *The Conflicts Between Strength and Toughness*

The quest for engineering materials that possess both high strength and toughness (damage tolerant) remains elusive. This emanates from the fact that the two properties are mutually exclusive. It is important to note that the mechanisms that promote high strength tend to oppose/conflict with those mechanisms that promote higher toughness. Strength sometimes represents a material resistance to nonrecoverable deformation (e.g. plastic deformation). On the other hand, toughness is a measure of the material’s resistance to fracture and, as such, requires a material’s ability to dissipate local high stress by enduring deformation (Zhu et al. 2015; Ritchie 2008, 2011). This explains the reason why hard materials tend to be brittle and lower strength materials (mostly metals), which can deform more readily, tend to be tougher (Ritchie 2011). It is interesting to note that much research efforts on hard and superhard materials have focused on pursuing higher strength with rather limited corresponding regard for toughness (Veprek 2013; Zhu et al. 2015).

The drive towards damage-tolerant materials is to be able to utilise the light-weight hard and superhard materials for vital, safety-critical applications such as in aerospace, transportation and power generation industries (Ritchie 2011). Although the conflicts between strength and toughness are very real, it has been proven that there exist ways to attain both properties in a single material through the presence of multiple plasticity and toughening mechanisms acting on differing length scales

(Ritchie 2011). A successful example is the development of bulk metallic glass (BMG)-based composites which are composed of a crystalline dendrite second phase in a BMG matrix which essentially promotes the formation of multiple shear bands leading to a strong and tough material (Ritchie 2011). Nature-inspired toughening mechanisms which involve both intrinsic and extrinsic toughening have been utilised to design and synthesise biomimetic structural materials (Zhu et al. 2015). Despite these efforts, there still exists rather limited success in attaining both strength and toughness in superhard materials which often require material-specific complicated and expensive processing routes hardly applicable to other materials (Zhu et al. 2015).

## 8 Wear of Superhard Materials

Superhard materials find use in tribological applications due to their high hardness, high-temperature stability and chemical inertness relative to metals (Olagnon et al. 2006). However during operations chipping by interrupted impacting increases wear thus higher toughness is required for these materials to survive greater wear. Wear of superhard ceramic materials is highly dependent on both operating conditions (normal load, velocity and temperature) and material properties (grain size, mechanical and thermal properties) (Shetty et al. 1985; Morrell 1985; Cohen 1985). Previous and ongoing studies have shown that wear of ceramics depends to a large extent on the ‘wear mode’ occurring at the machining onset (Olagnon et al. 2006). At low loads and relatively low temperatures, the wear mode is to a large extent controlled by the tribochemical reactions. On the other hand, at higher loads and higher temperatures, the dominant wear mode is mechanical wear occurring by propagation of cracks along grain boundaries resulting in microfracture within the material (Olagnon et al. 2006). In the latter case, the microstructure of the material is expected to play a more significant role than its chemical stability (Olagnon et al. 2006). This clearly highlights the interlink between the fracture toughness, rupture strength, hot hardness and materials’ tribological properties.

As highlighted before, hardness alone does not guarantee good wear or tribological properties in any material. It is clear that the trend now is towards development of newer materials possessing high toughness and hot hardness which implies good wear properties.

## 9 Thermal Shock

Most ceramic materials have low thermal conductivity thus making them prone to thermal shock which occurs as a result of a sudden change in temperature especially during cooling. This basically introduces transient thermal stresses which can



become large enough to induce damage such as microcracking or complete fracture (Fantozzi and Saadaoui 2014). Thermal shock can be quantified using the equation below:

$$\Delta T_c = \sigma_f \frac{(1 - \nu)}{E\alpha} \quad (3.17)$$

The value  $\Delta T_c$  is the applied temperature difference in quenching experiments often used as a thermal shock parameter indicating resistance to crack initiation. Here  $\sigma_f$  is the strength,  $\nu$  the Poisson's ratio,  $E$  is the Young's modulus and  $\alpha$  coefficient of thermal expansion.

Thus the thermal shock resistance is influenced in addition to specimen properties by material properties such as Young's modulus, thermal expansion coefficient, tensile strength and fracture toughness. It is thus apparent that increasing the crack resistance generally increases the material shock resistance. Typically, coarse grains induce a high crack growth resistance, thus maintaining a high initial strength which gradually decreases after thermal shock compared to the catastrophic strength loss observed in fine grain material (Fantozzi and Saadaoui 2014). The behaviour observed in fine grain materials is however not well understood and is open to debate. Thermal shock resistance of  $\text{Si}_3\text{N}_4$  ceramics has been enhanced by using SiC whisker reinforcement or by coarsening and elongating the microstructure (Lawn et al. 1994).

## 10 Concluding Remarks and Future Trends

In this chapter, the behaviour of hard, superhard and ultrahard materials has been analysed in relation with their microstructures. It has been shown that the development of superhard materials with hardness values approaching that of diamond can be elucidated through microstructural control. It is clear that the progress of these materials has been hindered owing to their inferior fracture toughness properties which basically limit their range of applications. A number of fracture enhancement techniques have been utilised such as grain bridging and transformation toughening through tailoring the microstructures. However there is still potential to create damage-tolerant superhard and ultrahard materials that can be utilised in safety-critical applications. The strength-fracture toughness conflict still remains elusive as these properties are mutually exclusive. Although efforts have been made to produce strong and tough materials (e.g. BMGs), there still remains scepticism whether the techniques utilised can be applied to other materials. The thermal and wear properties of hard, superhard and ultrahard materials form an important aspect as they directly affect the performance owing to their operating conditions (high temperature and interrupted impact). It has been shown that coarse-grained/elongated microstructures with greater resistance to crack initiation and propagation give the best performance at higher temperatures and impact. However this

happens at the expense of hardness. Thus there is a need to strike a balance between the two properties and hence form the future trends towards achieving more useful superhard materials rather than only superhardness. The present review is not meant to be completely exhaustive but to shed some light on the more important microstructural aspects which have a direct influence on a materials' performance.

## References

- Anderson PM, Li C (1995) Hall–Petch relations for multilayered materials. *Nanostruct Mater* 5:349
- Anstis GR et al (1981) *J Am Ceram Soc* 64:533–538
- Ashby MF (1972) *Acta Metall* 20:887
- Badzian AR (1981) Cubic boron nitride–diamond mixed crystals. *Mater Res Bull* 16 (11):1385–1393
- Barnett SA (1993) Physics of thin films. In: Francombe MH, Vossen JL (eds) *Mechanics and dielectric properties*, vol 17. Academic, Boston
- Brazhkin VV (2007) High pressure synthesized materials: treasure and hints. *High Pressure Res* 27 (3):333–351
- Brazhkin VV, Lyapin AG, Hemley RJ (2002) Harder than diamond: dreams and reality. *Philos Mag* A82(2):231–253
- Brazhkin V et al (2004) From our readers: What does ‘harder than diamond’ mean? *Nat Mater* 3:576–577
- Chen XQ et al (2011) Intrinsic correlation between hardness and elasticity in polycrystalline materials and bulk metallic glasses. *Intermetallics* 19:1275–1281
- Chu X et al (1992) Deposition and properties of polycrystalline TiN/NbN superlattice coatings. *J Vac Sci Technol A* 10:1604
- Cohen ML (1985) Calculation of bulk moduli of diamond and zinc-blende solids. *Phys Rev B* 32 (12):7988–7991
- Cottrell AH (1967) *An introduction to metallurgy*. Edward Arnold publishers, London, p 192
- Crampon J, Escaig BJ (1980) *Am Ceram Soc* 63:680
- Creyke WEC, Sainsbury IEJ, Morrell R (1982) Design with nonductile materials. Applied Science, London, pp 68–101, 115–133
- Davis L (1976) Metallic glasses. In: Gilman JJ, Leamy HJ (eds) *Fundamental Aspects of Structural Alloy Design*. Springer, US NY, p 431–450
- Decker BF, Kasper JS (1959) The crystal structure of a simple rhombohedral form boron. *Acta Crystallogr* 12:503–506
- Dubrovinskaia NA et al (1999) Thermal expansion and compressibility of Co W C. *J Alloys Compd* 285:242–245
- Elssner G et al (1999) *Ceramics and ceramic composites: materialographic preparation*. Elsevier, Amsterdam/New York, pp 144–158
- Evans AG (1974a) *Fracture mechanics of ceramics*, vol 1. Plenum Press, New York, p 17
- Evans AG (1974b) The role of inclusions in the fracture of ceramic materials. *J Mater Sci* 9:1145–1152
- Evans AG, Charles EA (1976) *J Am Ceram Soc* 59:371
- Evans AG, Lange FF (1975) *J Mater Sci* 10:1659–1664
- Fantozzi G, Saadaoui M (2014) Toughness, fatigue and thermal shock of ceramics: microstructural effects. *Compr Hard Mater* 2:299–319
- Frantsevich NH (1980) *Superhard materials*. Naukova Dumka: Kiev, Ukraine, 620
- Frischholz (2004) *Breviary Technical Ceramics*. Verband der Keramischen Industry e.V., Germany

- Gilman JJ (1973) Hardness – a strength microprobe. In: Westbrook JH, Conrad H (eds) The science of hardness testing and its research applications. American Society for Metals, Metals Park
- Gomez FJ, Elices M (2006) Fracture loads for ceramic samples with rounded notches. *Eng Fract Mech* 73(7):880–894
- Griffith AA (1920) Phenomena of rupture and flow in solids. *Philos Trans R Soc Lond A* 224:163–198
- Haines J et al (2001) Synthesis and design of superhard materials. *Annu Rev Mater Res* 31:1–23
- Helmersson U (1987) *J Appl Phys* 62:481
- Hertzberg RW (1989) Deformation and fracture mechanics of engineering materials, 3rd edn. Wiley, New York
- Hughes RE et al (1963) Structure of beta-rhombohedral boron. *J Am Chem Soc* 28(3):289–301
- Inoue A et al (1994) *Jpn Inst Met Mater Trans* 35:85
- Kelly JR (1995) Perspectives on strength. *Dent Mater* 11:103–110
- Kelly A, MacMillan NH (1986) Strong solids, 3rd edn. Clarendon, Oxford
- Knittle E et al (1995) High-pressure synthesis, characterization, and equation of state of cubic C-BN solid solutions. *Phys Rev B* 51(18):12149
- Koehler JS (1970) *Phys Rev B*:547
- Komatsu T et al (1996) Synthesis and characterization of a shock-synthesized cubic B–C–N solid solution of composition BC<sub>2</sub>5N. *J Mater Chem* 6(11):1799–1803
- Krstic VD (1984) Fracture of brittle solids in the presence of thermoelastic stresses. *J Am Ceram Soc* 67(9):589–593
- Krstic VD (1988) Grain-size dependence of fracture stress in anisotropic brittle solids. *J Mater Sci* 23:259–266
- Kurakevych OO (2009) Superhard phases and simple substances and binary compounds of the B–C–N–O system: from diamond to the latest results. *J Superhard Mater* 31(3):139–157
- Kurdumova V et al (1984) Polymorphous modifications of carbon and boron nitride. Naukova Dumka, Kiev
- Lambrecht WRL, Segall B (1993) Anomalous band-gap behaviour and phase stability of c-BN–diamond alloy. *Phys Rev B* 17(15):9289–9296
- Lange FF (1984) Structural ceramics: a question of fabrication reliability. *J Mater Eng Syst* 6:107–113
- Larsson M et al (1996) *Surf Coat Technol* 86/87:351
- Launey ME (2009) Fracture toughness and crack resistance curve behaviour in metallic glass matrix composites. *Appl Phys Lett* 94:241910–241913
- Launey ME, Buehler MJ, Ritchie RO (2010) On the mechanistic origins of toughness in bone. *Annu Rev Mater Res* 40:25–53
- Lawn BR, Swain MV, Phillips K (1975) *J Mater Sci Lett* 10:1236–1239
- Lawn BR et al (1994) Making ceramics ductile. *Science* 263:1114
- Leger JM et al (1994) Materials potentially harder than diamond: quenchable high-pressure phases of transition metal dioxides. *J Mater Sci Lett* 13:1688–1690
- Liu AY, Cohen ML (1989) Prediction of new compressibility solids. *Science* 245:841
- Liu A et al (1981) *Phys Rev B* 43:6742
- Lüthy H, White RA, Sherby OD (1979) *Mater Sci Eng* 39:211
- Malkow T (2001) Critical observations in the research of carbon nitride. *Mater Sci Eng* 302(2):311–324
- Matizanhuka WR (2010) A Study on the synthesis of ultrahard cubic BC<sub>2</sub>N heterodiamond. PhD Thesis, University of the Witwatersrand
- Mattesini M, Matar SF (2001) Search for ultra-hard materials: theoretical characterisation of novel orthorhombic BC<sub>2</sub>N crystals. *Int J Inorg Mater* 3:943–957
- Mcnamara D et al (2015) Fracture toughness evaluation of polycrystalline diamond as a function of microstructure. *Eng Fract Mech* 143:1–16
- Mohamed FA, Langdon TG (1974) *Metal Trans A* 5:2339

- Morrell R (1985) Handbook of properties of technical engineering ceramics part 1: an introduction for the engineer and designer. H.M.S.O, London, pp 92–93
- Mott N, Davis E (1979) Electron processes in non-crystalline materials. Clarendon Press, Oxford
- Munz D, Fett T (1999) Ceramics: mechanical properties, failure behaviour, materials selection, vol 36. Springer, Berlin, Heidelberg
- Nakano S (1996) Advanced materials '96: new trends in high pressure research. In: Proceedings of the 3rd NIRIM international symposium for advanced materials, National Institute for Research in Inorganic Materials, Japan, p 287
- Nakano S et al (1994) Segregate crystallisation of several diamond like phases from the graphitic BC<sub>2</sub>N without additive at 7.7GPa. Chem Mater 6(12):2246–2251
- Nalla RK, Kinney JH, Ritchie RO (2003) Mechanistic fracture criteria for the failure of human cortical bone. Nat Mater 2(3):164–168
- Niihara K et al (1982) J Mater Sci Lett 1:13–16
- Novikov V (1987) Physical properties of diamond. Naukova Dumka, Kiev. Kosolapova
- Oganov AR et al (2009) Ionic high pressure form of elemental boron. Nature 457:863–867
- Olagnon C, Chevalier J, Panchard V (2006) Global description of crack propagation in ceramics. J Eur Ceram Soc:1–9
- Pan Z et al (2005) Ab initio pseudopotential studies of cubic BC<sub>2</sub>N under high pressure. J Phys Condens Mater 17:3211–3220
- Pan Z et al (2006) *Ab initio* structural identification of high density cubic BC<sub>2</sub>N. Phys Rev B 73:214111–214114
- Pierson H (1994) Handbook of carbon, graphite, diamond and fullerenes: properties, processing and applications. Noyes Publications, New Jersey, pp 30–39
- Riedel R (1992) Materials harder than diamond? Adv Mater 4(11):759–761
- Riedel R (1994) Novel ultrahard materials. Adv Mater 6(7/8):549–560
- Ritchie RO (2008) Mechanisms of fatigue crack-propagation in metals, ceramics and composites: role of crack tip shielding. Mater Sci Eng A 103(1):15–28
- Ritchie RO (2011) The conflicts between strength and toughness. Nat Mater 10:817–822
- Ruoff A, Li TA (1995) Rev Mater Sci 25:249
- Schiotz J, Di Tolla ED, Jacobsen KW (1998) Nature 391:561
- Shetty DK et al (1981) Biaxial fracture studies of a glass-ceramic. J Am Ceram Soc 64(1):1–4
- Shetty DK et al (1985) J Mater Sci 20:1873–1882
- Shinn M, Hultman L, Barnett SA (1992) J Mater Res 7:901
- Solozhenko VL, Gregoryanz E (2005) Synthesis of superhard materials. Mater Today 8:44–51
- Solozhenko VL et al (2001) Synthesis of superhard cubic BC<sub>2</sub>N. Appl Phys Lett 78(10):1385.17
- Sun H et al (2001) Structural forms of cubic BC<sub>2</sub>N. Phys Rev B 64:094108-6
- Sung C-M, Sung M (1996) Carbon nitride and other speculative superhard materials. Mater Chem Phys 43:1–18
- Tateyama Y et al (1997) Proposed synthesis path for heterodiamond BC<sub>2</sub>N. Phys Rev B 55(16):R10161-4
- Taylor D (1996) Crack modelling: a technique for the fatigue design of components. Eng Fract Mech 3(2):129–136
- Taylor D (1999) Geometrical effects in fatigue: a unifying theoretical model. Int J Fract 21(5):413–420
- Taylor D (2004) Predicting the fracture strength of ceramic materials using the theory of critical distances. Eng Fract Mech 71(16–17):2407–2416
- Taylor D (2006) The theory of critical distances applied to the prediction of brittle fracture in metallic materials. Struct Integr Durab 1(2):145–154
- Taylor D, Cornetti P, Pugno N (2005) The fracture mechanics of finite crack extension. Eng Fract Mech 72(7):1021–1038
- Teter DM, Hemeley RJ (1996) Low compressibility carbon nitrides. Science 271:1161
- Tian Y (2012) Microscopic theory of hardness and design of novel superhard crystals. Int J Refract Met Hard Mater 33:93–106

- Veprek S (1999) The search for novel, superhard materials. *J Vac Sci Technol A* 17(5):2401–2420
- Veprek S (2013) Recent search for new superhard materials: go nano. *J Vac Sci Technol A* 5 (050822):1–33
- Veprek S, Argon AS (2001) Mechanical Properties of superhard nanocomposites. *Surf Coat Technol* 146–147:175–182
- Weiner S, Wagner HD (1998) The material bone: structural-mechanical functional relations. *Annu Rev Mater Sci* 28:271–298
- Widany J et al (1998) Density-functional based tight-binding calculations on zinc-blende type  $BC_2N$ -crystals. *Diam Relat Mater* 7:1633–1638
- Zerr A, Riedel R (2000) In: Riedel R (ed) *Handbook of ceramic hard materials*, vol 1. Wiley-VCH, Weinheim
- Zhao Y et al (2002) Superhard B–C–N materials synthesized in nanostructured bulks. *J Mater Res* 17(12):3139–3145
- Zheng JC et al (1999) Ground-state properties of cubic C–BN solid solutions. *J Phys Condens Mater* 11:927–935
- Zhu H et al (2015) Anomalous scaling law of strength and toughness of cellulose nanopaper. *Proc Natl Acad Sci USA* 112:1–6